Reports

Atomic Force Microscope Studies of Fullerene Films: Highly Stable C_{60} fcc (311) Free Surfaces

ERIC J. SNYDER, MARK S. ANDERSON, WILLIAM M. TONG, R. STANLEY WILLIAMS,* SAMIR J. ANZ, MARCOS M. ALVAREZ, YVES RUBIN, FRANÇOIS N. DIEDERICH, ROBERT L. WHETTEN

Atomic force microscopy and x-ray diffractometry were used to study 1500 Å–thick films of pure C_{60} grown by sublimation in ultrahigh vacuum onto a CaF_2 (111) substrate. Topographs of the films did not reveal the expected close-packed structures, but they showed instead large regions that correspond to a face-centered cubic (311) surface and distortions of this surface. The open (311) structure may have a relatively low free energy because the low packing density contributes to a high entropy of the exposed surface.

THE DISCOVERY OF A METHOD OF preparing macroscopic quantities of the pure carbon molecule C_{60} (buckminsterfullerene) has stimulated numerous studies to determine the bulk and surface structures of the condensed phases of this molecular material (*1–6*). To date, the surface structural studies have primarily emphasized films consisting of from one to a few monolayers of molecules. Such films of C_{60} molecules are readily deposited onto a substrate by evaporation of a benzene solution (*4*) or by sublimation in a vacuum chamber (*3, 5, 6*) and are relatively stable in air at room temperature. Scanning tunneling microscope (STM) studies of films of mixed fullerenes on graphite (*4*) and monolayer films of C_{60} on gold (111) surfaces (*5*) have both revealed close-packed structures, and a slightly distorted close-packed array of C_{60} molecules was observed on GaAs (110) (*6*). However, in these cases the molecular ordering was strongly influenced by the substrates because the films were so thin. In this report, we present the results of x-ray diffractometry (XRD) and atomic force microscopy (AFM) studies of 1500 Å–thick films of pure C_{60} grown by sublimation on CaF_2 (111) substrates, which were chosen because their symmetry and lattice spacing are compatible with close-packed C_{60} planes (*3*). In contrast to the results reported on the thinner films, we did not observe any close-packed structures but rather more open surfaces that correspond to a face-centered cubic (fcc) (311) plane.

The initial carbon fullerene material for the growth of the C_{60} films was prepared by the Krätschmer-Huffman method (*1*). This C_{60}-rich starting material was then purified to 99.95% by column chromatography (*2*). The substrates were CaF_2 (111) wafers etched with an HF solution saturated with CaF_2 and then rinsed with acetone. The films were grown by sublimation at the rate of one C_{60} monolayer per minute in ultrahigh vacuum onto room temperature substrates (*3*). The C_{60} films were typically about 1500 Å thick, as determined by a profilometer. These films were then subjected to two ex situ analyses: XRD and AFM. An AFM was required to study the surface morphology of the thicker fullerene films because their high resistivity made STM studies impractical.

The x-ray diffraction measurements of the C_{60} films were made with a Norelco 2θ powder diffractometer with a Cu x-ray source. The XRD patterns revealed that all the pure C_{60} films used in this study were polycrystalline, in contrast to the primarily (111) oriented films deposited by subliming a mixture of fullerenes (*3*). All the XRD patterns contained the three major peaks that were indexed to a hexagonal close-packed (hcp) lattice in the powder samples of Krätschmer *et al.* (*1*), but we have assigned the peaks to reflections from an fcc lattice. An example of an XRD pattern of a 1500 Å C_{60} thin film is shown in Fig. 1 and summarized in Table 1. The fact that our *d*-spacings were smaller than those of Krätschmer *et al.* (*1*) probably resulted from the smaller C_{70} contamination in our films, since we have observed that mixed-fullerene films exhibit a larger lattice constant (*3*). From the 2θ values of the XRD peaks, we determined that the intermolecular C_{60} spacing in the film was 9.80 ± 0.01 Å, and from the peak widths we obtained the correlation length (*7*) perpendicular to the substrate surface for each crystallite orientation, as listed in Table 1.

The AFM investigations of the C_{60} films were made in air at room temperature with a Digital Instruments Nanoscope II atomic force microscope. The AFM cantilevers, which were also supplied by Digital Instruments, had 100-μm silicon nitride tips (*8*). Several cantilevers were used in these experiments in order to achieve image resolution of the order of 1 to 10 Å. In each case, the cantilever was initially lowered to and scanned over a 100 nm by 100 nm area of the sample at a force setpoint of about 10 nN. The feedback gain parameters were then adjusted in the single line scan mode to minimize the noise in the AFM signal. The scan size was then enlarged to about 1 μm on a side and then slowly lowered back down to 50 nm or less. None of the features in the topographs changed when the scan

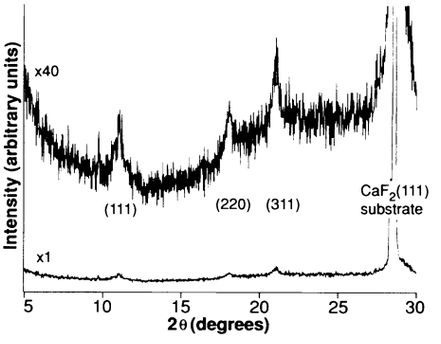

Fig. 1. X-ray diffraction pattern of a 1500 Å film of pure C_{60} on a CaF_2 (111) substrate. The peaks from the film are labeled according to reflections from an fcc lattice.

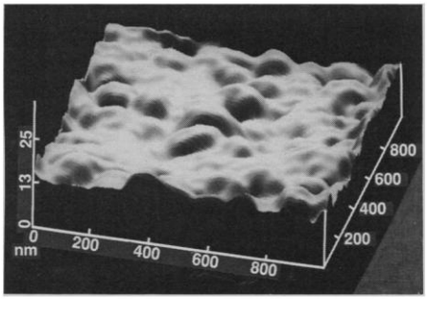

Fig. 2. AFM topograph of a C_{60} film on a CaF_2 (111) substrate. The scan dimensions are 1 μm on each side. The scale perpendicular to the surface is expanded by a factor of 12 compared to the scale parallel to the surface, which makes the surface appear to be much rougher than it actually is.

E. J. Snyder, W. M. Tong, R. S. Williams, S. J. Anz, M. M. Alvarez, R. L. Whetten, Department of Chemistry and Biochemistry, and Solid State Science Center, University of California, Los Angeles, CA 90024.
M. S. Anderson, Jet Propulsion Laboratory, Pasadena, CA 91109.
Y. Rubin and F. N. Diederich, Department of Chemistry and Biochemistry, University of California, Los Angeles, CA 90024.

Table 1. X-ray diffraction results for C_{60} films. The reflections were indexed (002), (110), and (112) for an hcp lattice by Krätschmer *et al.* (*1*).

Reflection (fcc)	2θ (degrees)		*d*-spacing (Å)		Correlation length (Å)
	This work	(*1*)	This work	(*1*)	
(111)	11.1 ± 0.05	(10.81)	7.98	(8.18)	120 ± 15
(220)	18.1 ± 0.05	(17.69)	4.90	(5.01)	120 ± 15
(311)	21.1 ± 0.05	(20.73)	4.22	(4.27)	250 ± 70

rate was changed. All images presented here were photographed off the video monitor; they were slightly smoothed to remove sharp noise spikes, but not frequency filtered or stretched to force agreement with any preconceptions of the symmetry of the surfaces.

The largest scale surface features scanned with the AFM (1 μm by 1 μm), shown in Fig. 2, were reproducible and similar to results reported elsewhere from STM studies (*5*). The AFM topographs were characterized by rounded and gently sloping hillocks, rather than by the inclined flat faces characteristic of a faceted surface. The typical lateral size of the hillocks was 500 to 2500 Å and the base to top heights were 100 to 250 Å, which correspond to a maximum thickness variation of the film of about 15%. Hillocks were never observed on uncoated substrates and they did not change with repeated scanning of the AFM.

At moderate scan sizes (<1000 Å), topographs with various types of row-like features were observed. In Fig. 3A, we show an ordered row-like surface pattern with corrugation within the rows, whereas Fig. 3B reveals a similar image but with a less ordered pattern (the orientation of the rows is rotated by 90° in the two topographs). The typical row-to-row separation in Fig. 3A is about 15 Å and did not change with scan frequency. The discrete features in the rows in Fig. 3, A and B, had a center-to-center spacing of 9 to 10 Å along the rows and thus appear to be individual C_{60} molecules. The molecules did not form a close-packed array, as reported in the STM studies of the monolayer films (*4–6*), in any of the topographs collected.

The highly ordered row structures of Fig. 3A were observed only at the tops of the hillocks such as those in Fig. 2, whereas less ordered row-like structures were observed on the curved sides of the hillocks. We compared the observed structures to several possible high-index surfaces (*9*) of solid C_{60} based on fcc, hcp, and bcc (body-centered cubic) packing of the molecules. Only the hcp (112) and the fcc (311) surfaces came close to matching the observed structures. Given the 9.8 Å van der Waals diameter of the C_{60} molecules determined from the x-ray data, the row separations for the hcp (112) and fcc (311) surfaces should be 20 Å and 15.8 Å, respectively. Since only the latter value is within the experimental error of the observed row spacing, we have assigned the structure of Fig. 3A to the fcc (311) surface. This corresponds to one of the crystallite orientations parallel to the substrate that produced the (311) reflection in the XRD pattern of Fig. 1. In Fig. 4, we show a schematic diagram of the fcc (311) unit cell, and in Fig. 5 we have superimposed the unit cell outline on top of a gray-scale AFM image of the C_{60} surface.

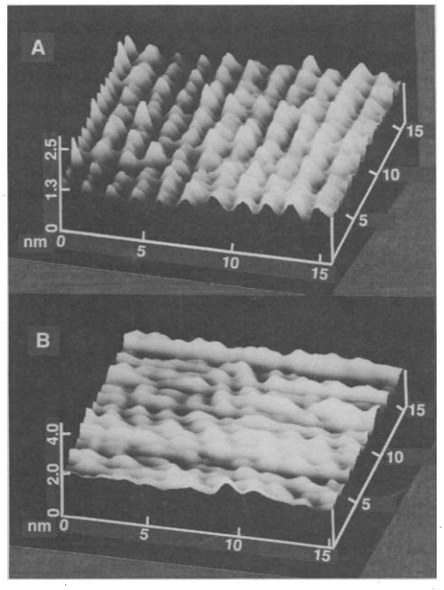

Fig. 3. High resolution AFM topographs of a C_{60} film showing row-like structures with scan dimensions 150 Å on each side. (**A**) From the top of a hillock such as those in Fig. 2. (**B**) From the side of a hillock.

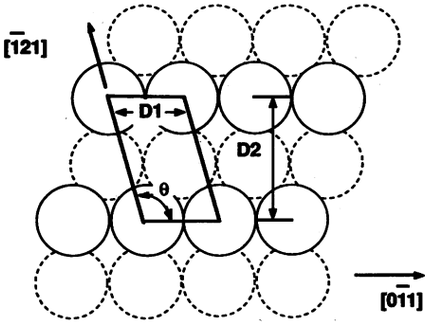

Fig. 4. Schematic drawing of an ideal fcc (311) surface of solid C_{60}, where the distances D1 and D2 are 9.8 Å and 15.8 Å and the angle (θ) is 106.78°.

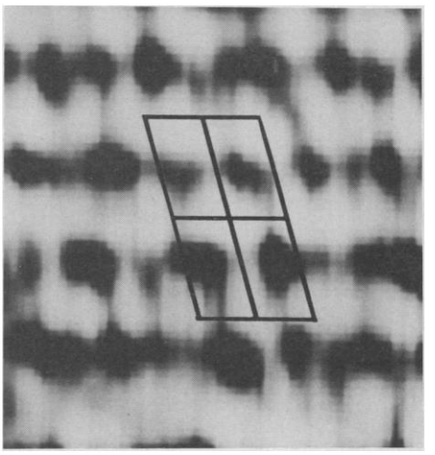

Fig. 5. An expanded gray-scale image of the row structure of Fig. 3A. In this case, the viewpoint is directly overhead. The dark lines show the boundaries of four ideal (311) unit cells superimposed over the image. This image is only lightly smoothed and not frequency filtered.

Krätschmer *et al.* (*1*) originally assigned a hexagonal structure to solid C_{60} despite the absence of the hcp (101) peak, which is a strong reflection, from their XRD pattern. Other researchers (*10–12*) have subsequently assigned a cubic structure to bulk C_{60}. The fact that the fcc (200) peak was missing from the XRD patterns is the result of a coincidental vanishing of the molecular form factor for (n00) reflections, where n is an even number (*11, 12*). Our observations are a further confirmation of the fcc structure of C_{60} films.

The surface (311) planes are relatively undistorted on top of the hillock features shown in Fig. 2, presumably because they are parallel to the (311) planes of the underlying material. Instead of exposing other recognizable crystal faces, the sides of the hillocks display row-like patterns and spacings that are similar to a (311) surface, but the rows are not as straight and there is more disorder in the molecular arrangement. Thus, the planes that are exposed on the slopes appear to reconstruct to form an open surface structure, rather than close-packed arrays.

The x-ray correlation length for crystallites with (311) orientations is significantly longer than those with (110) and (111) orientations (Table 1), but all three correlation lengths are significantly shorter than the film thickness. Thus, none of the orienta-

tions yields crystallites that coherently span the entire thickness of the film. However, the (311) layers are apparently stacked with fewer defects during growth than the other planes, even though the CaF_2 (111) substrate was chosen to provide a lattice-matched template for the close-packed planes of C_{60} (*3*). The preference for (311) planes in the films could be because they are thermodynamically more stable or they are kinetically favored and simply grow faster than the other orientations.

The rolling hillock morphology revealed in Fig. 2 resembles that of amorphous surfaces, such as those formed by the sputtering of graphite (*13*), rather than the faceted surface of a polycrystalline film. The kinetics of the formation of hillocks has been explained in terms of the competition between the stochastic arrival of deposited particles, which leads to a totally random structure, and the diffusion of particles on the surface, which leads to correlation of the features on the surface (*13, 14*). For the extremely low deposition rates of the C_{60} films grown for this study, the morphology of the films should be determined primarily by surface diffusion. Since room temperature represents a very high temperature for the weakly bonded C_{60} molecules, the exposed surfaces should be close to thermodynamic equilibrium structures.

A thermodynamically stable (311) orientation for the exposed surface is completely counterintuitive. The lowest energy surface for an fcc solid should be a (111) plane, whereas the (311) is normally a relatively high energy surface (*15*). We propose that the fcc (311) surface of solid C_{60} is stabilized relative to the (111) close-packed surface at room temperature because of the higher entropy afforded by the more open surface. With its large moment of inertia and spherical shape, C_{60} rotates in its bulk crystal lattice sites down to at least 100 K (*16*). The row separations in the (311) surface reduce the number of nearest neighbors in the surface plane from six to two compared to a close-packed surface and thus may allow less hindered rotations of the molecules at the surface. In addition, a more open structure allows more disorder in the rows, as observed in Fig. 3, A and B. This entropy gain could lower the surface free energy of the (311) plane relative to the close-packed surface and thus stabilize the (311) surface at room temperature.

Since the forces among C_{60} molecules are primarily van der Waals in nature, there is a great temptation to regard the solid as a noble gas ice in which the individual "atoms" have a mass of 720 AMU. Indeed, solid Ne, Ar, Kr, and Xe all have the fcc structure, and solid C_{60} appears to continue that trend. However, the large number of internal degrees of freedom in C_{60} makes any intuition based upon the packing of atoms in a crystal lattice tenuous at best. The fact that the free surfaces of our C_{60} films have an open (311) structure that is stable with respect to scanning with an AFM tip may be a manifestation of the internal structure of these nominally spherical molecules and the role that entropy plays in stacking the molecules.

REFERENCES AND NOTES

1. W. Krätschmer, L. D. Lamb, K. Fostiropoulos, D. R. Huffman, *Nature* **347**, 354 (1990).
2. H. Ajie *et al.*, *J. Phys. Chem.* **94**, 8630 (1990).
3. W. M. Tong *et al.*, *ibid.*, **95**, 4709 (1991).
4. J. L. Wragg, J. E. Chamberlain, H. W. White, W. Krätschmer, D. R. Huffman, *Nature* **348**, 623 (1990).
5. R. J. Wilson *et al.*, *ibid.*, p. 621.
6. Y. Z. Li *et al.*, *Science* **252**, 547 (1991).
7. A. Guinier, *X-Ray Diffraction* (Freeman, San Francisco, 1963), pp. 121–125.
8. T. R. Albrecht and C. F. Quate, *J. Vac. Sci. Technol* **A6**, 271 (1988).
9. J. F. Nicholas, *An Atlas of Models of Crystal Surfaces* (Gordon and Breach, New York, 1965).
10. R. M. Fleming *et al.*, *Mat. Res. Soc. Proc.*, in press.
11. P. A. Heiney *et al.*, *Phys. Rev. Lett.* **66**, 2911, (1991).
12. J. E. Fischer *et al.*, *Science* **252**, 547 (1991).
13. E. A. Eklund, R. Briunsma, J. Rudnick, R. S. Williams, in preparation.
14. G. S. Bales *et al.*, *Science* **249**, 264, (1990).
15. A. Zangwill, *Physics at Surfaces* (University Press, Cambridge, 1988), p. 14.
16. C. S. Yannoni, R. D. Johnson, G. Meijer, D. S. Bethune, J. R. Salem, *J. Phys. Chem.* **95**, 9 (1991).

17. This work was supported in part by the Office of Naval Research (E.J.S., W.M.T., and R.S.W.) and the National Science Foundation (S.J.A., M.M.A., Y.R., F.N.D., and R.L.W.). Some of the work described in this paper was carried out at the Jet Propulsion Laboratory, California Institute of Technology through an agreement with the National Aeronautical and Space Administration.

29 April 1991; accepted 10 June 1991

Field-Induced Nanometer- to Atomic-Scale Manipulation of Silicon Surfaces with the STM

IN-WHAN LYO AND PHAEDON AVOURIS

The controlled manipulation of silicon at the nanometer scale will facilitate the fabrication of new types of electronic devices. The scanning tunneling microscope (STM) can be used to manipulate strongly bound silicon atoms or clusters at room temperature. Specifically, by using a combination of electrostatic and chemical forces, surface atoms can be removed and deposited on the STM tip. The tip can then move to a predetermined surface site, and the atom or cluster can be redeposited. The magnitude of such forces and the amount of material removed can be controlled by applying voltage pulses at different tip-surface separations.

THERE HAS BEEN A CONTINUING EFFORT to find ways to manipulate materials at ever decreasing length scales. The ability of the STM to address and probe individual surface sites makes it a promising tool for the manipulation of materials on the nanometer scale (*1*). In particular, soon after the development of the STM (*2*) the possibility of transferring material between the tip and the sample was discussed (*3*). Early work established that voltage pulses applied to the STM tip can lead to the deposition of material on the sample surface (*4, 5*), while in other cases (*6, 7*) pits were created on the surface. The early work was exploratory, and the mechanisms by which the surface modifications took place were not established. However, in two recent STM studies involving desorption of adsorbates from silicon (*8*) and deposition of gold particles from a god tip (*9*), the strong electric fields that can develop between the tip and the sample were invoked. Similarly, the field enhancement of adsorbate diffusion processes (*8, 10*) was suggested.

We show that even the strongly and covalently bonded silicon substrate atoms can be manipulated with the STM, and we analyze the mechanisms by which this is accomplished. Specifically, by combining the effects of the strong electric field formed between the STM tip and the surface with chemical tip-sample interactions, we reproducibly transfer Si atoms and Si clusters up to tens of atoms from the surface to the tip. Moreover, we could then redeposit these clusters or atoms at predetermined sites of the surface. The mechanism involves a field-evaporation process with a low-threshold field that is modified by chemical and mechanical tip-sample interactions. The STM used in these studies as well as of the techniques used in sample preparation have been described previously (*11*).

Field evaporation involves the ionization and desorption of individual atoms or clus-

IBM Research Division, T. J. Watson Research Center, Yorktown Heights, NY 10598.